Tensile Stress-Dependant Fracture Behavior and Its Influences on Photovoltaic Characteristics in Flexible PbS/CdS Thin Film Solar Cells

ARTICLE *in* ACS APPLIED MATERIALS & INTERFACES · FEBRUARY 2015

Impact Factor: 6.72 · DOI: 10.1021/am507301c · Source: PubMed

4 AUTHORS, INCLUDING:

Seung Min Lee
Yonsei University
12 PUBLICATIONS **31** CITATIONS
SEE PROFILE

Bhaskar Chandra Mohanty
Thapar University
38 PUBLICATIONS **236** CITATIONS
SEE PROFILE

ACS APPLIED MATERIALS & INTERFACES

Research Article

www.acsami.org

Tensile Stress-Dependent Fracture Behavior and Its Influences on Photovoltaic Characteristics in Flexible PbS/CdS Thin-Film Solar Cells

Seung Min Lee,[†,§] Deuk Ho Yeon,[†,§] Bhaskar Chandra Mohanty,[‡] and Yong Soo Cho*[,†]

[†]Department of Materials Science and Engineering, Yonsei University, Seoul 120-749, Korea

[‡]School of Physics & Materials Science, Thapar University, Patiala, 147004, India

Supporting Information

ABSTRACT: Tensile stress-dependent fracture behavior of flexible PbS/CdS heterojunction thin-film solar cells on indium tin oxide-coated polyethylene terephthalate (PET) substrates is investigated in terms of the variations of fracture parameters with applied strains and their influences on photovoltaic properties. The PbS absorber layer that exhibits only mechanical cracks within the applied strain range from ∼0.67 to 1.33% is prepared by chemical bath deposition at different temperatures of 50, 70, and 90 °C. The PbS thin films prepared at 50 °C demonstrate better mechanical resistance against the applied bending strain with the highest crack initiating bending strain of ∼1.14% and the lowest saturated crack density of 0.036 μm^{-1}. Photovoltaic properties of the cells depend on the deposition temperature and the level of applied tensile stress. The values of short-circuit current density and fill factor are dramatically reduced above a certain level of applied strain, while open-circuit voltage is nearly maintained. The dependency of photovoltaic properties on the progress of fractures is understood as related to the reduced fracture energy and toughness, which is limitedly controllable by microstructural features of the absorber layer.

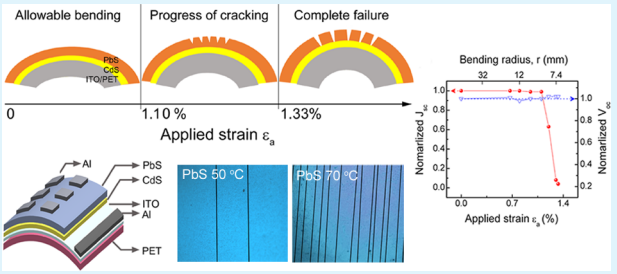

KEYWORDS: *lead sulfide, chemical bath deposition, flexible solar cell, fracture behavior*

INTRODUCTION

Photovoltaic cells on flexible polymer substrates have been investigated over the past decade because of their great potential for extended applications including as a mobile energy source. Particularly, the choice of absorber layer for the flexible substrate is very limited since the absorber layer needs to be processed below the softening point of the polymeric substrates. Several organic absorber materials, such as poly(3-hexylthiophene) (P3HT) and poly[2-methoxy-5-(2-ethylhexyloxy)-1,4-phenylenevinylene] (MEH-PPV), may be suitable for the flexible applications, but the practical utilization is very limited due to their compatibility issue with polymer substrates and their poor intrinsic long-term stability.[1,2] On the other hand, typical inorganic absorbers for thin-film solar cells, including Cu(In,Ga)Se_2 and CdTe, have been actively studied for the flexible applications.[3−5] The selection of substrates for the inorganic absorber is critical since it determines maximum processing temperature for the synthesis and densification of the absorber materials. Only highly thermal resistive substrates including metal foils have been considered as an ideal choice for the inorganic absorbers demanding at least 500 °C for densification to cover the broader range of applications potentially favoring lower softening temperature-polymer substrates including polyethylene terephthalate (PET), poly(ether sulfone) (PES) and polyethylene naphthalate (PEN); however, nonconventional absorber-driven cell structures that are processable below 100 °C are preferred.

Lead sulfide (PbS) has drawn considerable interest as one of the rare p-type absorbers for thin-film solar cells due to its high absorption coefficient of ∼1 × 10^5 cm^{-1} in the visible light and adjustable band gap toward a higher value (>1.3 eV) suitable for better band alignment in typical cell structures.[6−8] There has been no report concerning the deposition of PbS thin films on any flexible polymer substrate even though polycrystalline PbS can be easily formed at temperature below 100 °C by the known chemical bath deposition (CBD) process. There are several reports on the PbS/CdS heterojunction thin-film photovoltaic cells fabricated by CBD on a rigid glass substrate.[9−11]

In the meantime, there have been extensive studies on mechanical or fracture behavior of thin films deposited onto polymer substrates for a variety of flexible electronic devices.[12−14] Cracks or macrodefects developed on the surface of thin films as a result of externally applied stress are regarded as the reason for substantial degradation of the devices' functional performance.[15] In the field of flexible thin-film solar cells, surprisingly, there have been no systematic studies about the fracture behavior under tensile stress even though there is a rare report proposing that the photovoltaic performance of Cu(In,Ga)Se_2 cells can be critically affected by flexibility stress and mechanical cycling.[5]

Received: October 21, 2014
Accepted: February 9, 2015
Published: February 9, 2015

DOI: 10.1021/am507301c
ACS Appl. Mater. Interfaces 2015, 7, 4573−4578

In this work, PbS/CdS thin-film solar cells fabricated at <100 °C on a PET substrate are demonstrated as an example of low-temperature processable flexible solar cells and for the investigation of fracture behavior under various stress conditions. Only the crystallite size of PbS was intentionally changed for higher photovoltaic properties and also as a critical parameter in minimizing unwanted fracture degradation of the PbS layer. The sensitivity of the photovoltaic performance to the applied strain ε_a (or bending radius) is quantitatively described with calculated parameters of the saturated crack density ρ_s and crack initiating critical strain ε_c.

EXPERIMENTAL SECTION

Al/PbS/CdS/indium tin oxide (ITO)/PET solar cells with a cell area of ~0.09 cm^2 were fabricated. For the substrate, an ITO (~100 nm)-coated PET substrate possessing a sheet resistance of ~30 Ω/square with a thickness of 175 μm was used. The substrate was cleaned in acetone and deionized water for 10 min each by ultrasonic agitation. CdS thin films were first deposited onto the cleaned ITO/PET substrate by CBD. The deposition was carried out under magnetic stirring in an aqueous solution containing 0.025 M cadmium nitrate ($Cd(NO_3)_2 \cdot 4H_2O$, 98%; Kanto Chemical Co., Ltd., Tokyo, Japan), 0.15 M sodium citrate ($Na_3C_6H_5O_7$, 99%; Duksan, Korea), 0.3 M ammonia (NH_3, 25%; Duksan, Korea), and 0.05 M thiourea (CH_4N_2S, 99%; Sigma-Aldrich, St. Louis, MO, USA). The deposition process was performed at 80 °C, while the substrate was dipped into the solution for 15 min. The process was repeated twice to obtain a CdS thickness of ~50 nm.

As a next step, PbS film was deposited onto the CdS film by the CBD method in an aqueous solution containing 0.05 M lead nitrate ($Pb(NO_3)_2$, 99.3%; Kanto Chemical Co., Ltd., Japan), 0.04 M triethanolamine ($C_6H_{15}NO_3$, 99%; Aldrich, Milwaukee, WI), 0.2 M sodium hydroxide (NaOH, 95%; Duksan, Korea), and 0.06 M thiourea. The films were grown at different temperatures of 50, 70, and 90 °C for 50, 20, and 4 min, respectively, to obtain an identical PbS thickness of ~350 nm at each temperature. After the PbS deposition, the as-deposited films were rinsed in deionized water and finally dried in N_2 gas. An Al top electrode with a thickness of ~100 nm was deposited by thermal evaporation.

Surface morphology and cross-sectional images of the films were obtained by field emission scanning electron microscopy (FESEM: JSM-7001F, JEOL, Japan). Current density–voltage (J–V) measurements were recorded at room temperature under AM 1.5 illumination using an I–V curve analyzer (IviumStat, Ivium Technology, USA) and a solar simulator (Sun 2000, ABET technology, USA).

Figure 1a shows a schematic illustration of the prepared flexible solar cells consisting of PbS/CdS heterojunction thin films. Flexibility was evaluated by bending the flexible cells and thus by applying tensile stress to the flexible structure as depicted in Figure 1b. The bending evaluation method is similar to that used for ZnO thin films in our earlier studies.[12,13] The sample was loaded in a fixture between two parallel holders. One of the holders was attached to a micrometer so that the bending radius was adjusted precisely. As one holder was moved by using the micrometer, the sample was gradually bent into a sinusoidal shape. Since the estimated Young's modulus of the thin-film structure ($E_f \approx 77.0$ GPa) is far larger than that of the substrate (E_s = 2.3 GPa),[16] the neutral surface shifts toward the film side. In such case, the induced strain at the top of the film can be given as[17,18]

$$\varepsilon_a = \left(\frac{t_f + t_s}{2R}\right)\frac{(1 + 2\eta + \chi\eta^2)}{(1 + \eta)(1 + \chi\eta)} \quad (1)$$

where t_f and t_s are the thicknesses of the film and substrate, respectively, $\eta = t_f/t_s$, $\chi = E_f/E_s$, and R is the radius of curvature of the center of the bent sample. The values of R were calculated using a formula given elsewhere.[19] The value of E_f was estimated by using a known mixing rule of Young's modulus for the Al, PbS, CdS, and ITO layers with the thickness of each layer.[20] The reported Young's modulus values of 70.0, 70.2, 61.1, and 116 GPa were used for Al, PbS, CdS, and ITO, respectively.[21−24]

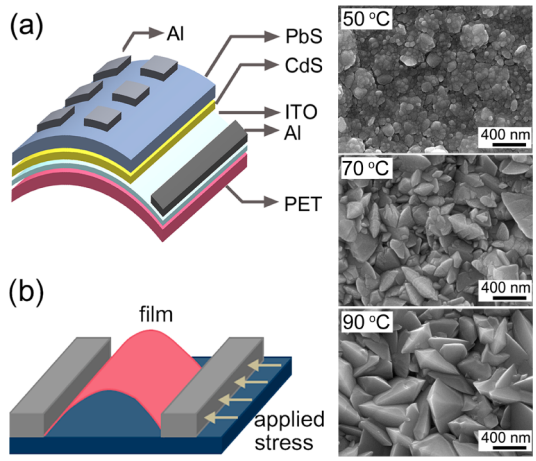

Figure 1. Schematic illustrations of (a) PbS/CdS heterojunction thin-film solar cell structure on PET substrate and (b) a setup for the flexibility evaluation of the cells. SEM surface images of PbS films processed at different deposition temperatures of 50, 70, and 90 °C are presented.

The image of fracture evolution in the center of the bent sample was recorded in situ by an optical microscope (LV150 BD DIC, Nikon, Japan). The fracture behavior was expressed in terms of the number of cracks generated. The analysis of the fracture behavior is truly based on the number of linear cracks fully developed across the samples perpendicular to the bending direction as studied elsewhere.[12,15,18] Other local defects possibly present on the film surface were not considered. The variations of the photovoltaic properties were measured as a function of the applied strain to correlate with the stress-dependent fracture behavior. The photovoltaic properties were measured after the specific bending strain was applied for 10 s and then released.

RESULTS AND DISCUSSION

Figure 1 also represents surface microstructures of the PbS thin films deposited onto flexible substrates at different temperatures of 50, 70, and 90 °C. The temperature range applied in this study is very typical for synthesizing PbS crystallites, as reported in the CBD method for PbS thin films.[9,10] As expected, the morphologies of the surface strongly depended on the processing temperature. A dense microstructure consisting of smaller grains is evident at the lowest temperature of 50 °C. When the deposition temperature was increased to 90 °C, the surface morphology changed into a large faceted-grain microstructure. A high temperature yields high decomposition rates of each precursor into Pb and S ions, resulting eventually in facilitating crystal growth. X-ray diffraction patterns of the films (not presented here) revealed polycrystalline nature. The main peaks including (200) and (220) planes significantly increased with increasing processing temperature, confirming that the crystallinity was enhanced dominantly by the processing temperature.

Figure 2 shows the current density–voltage curves of the resultant solar cells processed at different deposition temperature for the PbS layer. The quantitative values of short-circuit current density J_{sc}, open-circuit voltage V_{oc}, fill factor FF, and conversion efficiency η are listed in the inserted Table of Figure 2. Standard deviations of the parameters over the multiple measurements are provided in Supporting Information, Table 1S. The best efficiency of ~1.01% with the values of 11.90 mA/

DOI: 10.1021/am507301c
ACS Appl. Mater. Interfaces 2015, 7, 4573−4578

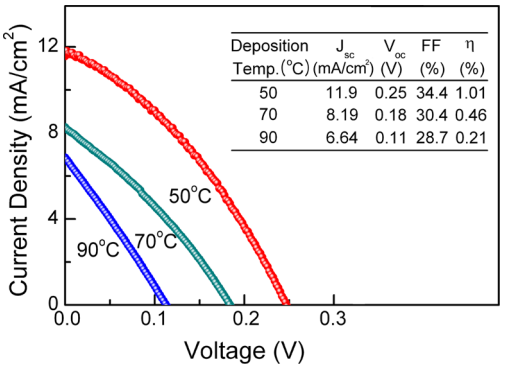

Deposition Temp. (°C)	J_{sc} (mA/cm^2)	V_{oc} (V)	FF (%)	η (%)
50	11.9	0.25	34.4	1.01
70	8.19	0.18	30.4	0.46
90	6.64	0.11	28.7	0.21

Figure 2. $J-V$ curves of flexible PbS/CdS solar cells processed at different deposition temperatures of 50, 70, and 90 °C for the PbS absorber layer. The standard deviations of photovoltaic parameters are provided in the Supporting Information, Table 1S.

cm^2 for J_{sc}, 0.25 V for V_{oc}, and 34.4% for FF was obtained for the PbS absorber prepared at 50 °C. When the PbS deposition temperature was increased to 90 °C, a lower conversion efficiency of ∼0.21% was achieved with 6.64 mA/cm^2 for J_{sc}, 0.11 V for V_{oc}, and 28.7% for FF. The tendency of increasing photovoltaic performance with decreasing deposition temperature can be attributed mainly to the smaller crystallite size induced at lower processing temperature, which leads to a wider band gap and potentially favorable band alignment between PbS and CdS layers.[11] There is no clear explanation available for the crystallite size dependence of the band gap for the larger crystallite sizes beyond the quantum confinement range of 5−18 nm. Several factors such as residual stress, defects, grain size, and morphology may potentially affect the band gap.[25,26] It is also conjectured that the larger grains of PbS leave more effective unfilled intergranular volume so that the absorption per unit thickness is reduced, while they may also induce the localized energy states from defects in grains and grain boundaries, resulting in a lowered band gap.[11]

Tensile stress-driven flexibility of the PbS films deposited at different temperatures was evaluated to define the fracture behavior, that is, crack initiation and propagation. All films showed resistance to crack initiation up to a certain critical value of applied strain ε_c. When the applied strain exceeded the critical strain ε_c, cracks perpendicular to the tensile stress axis were generated. The level of crack density ρ is defined as the number of parallel cracks per unit length. The crack density increases with applied strain, then saturates asymptotically, but also depending on the location of the sample. The central portion of the films showed a higher density of cracks compared to the regions away from the center, which indicates nonuniform strain distribution in the films due to the nature of the bending evaluation. This work focuses only on the central region where the strain is believed to be uniform and intensified.

Figure 3 shows the in situ optical microscopy images of the PbS films after applying an identical strain ε_a of ∼1.20%. The micrographs were photoedited in blue backgrounds for better contrast visualization. The 50 °C-processed film shows the lowest crack density on surface. As the deposition temperature increased to 90 °C, the crack density increased by demonstrating more perpendicular cracks with the substantial reduction in average spacing between the adjacent cracks. According to the surface SEM observation (not shown here), the cracks on surface became more apparent with a larger width

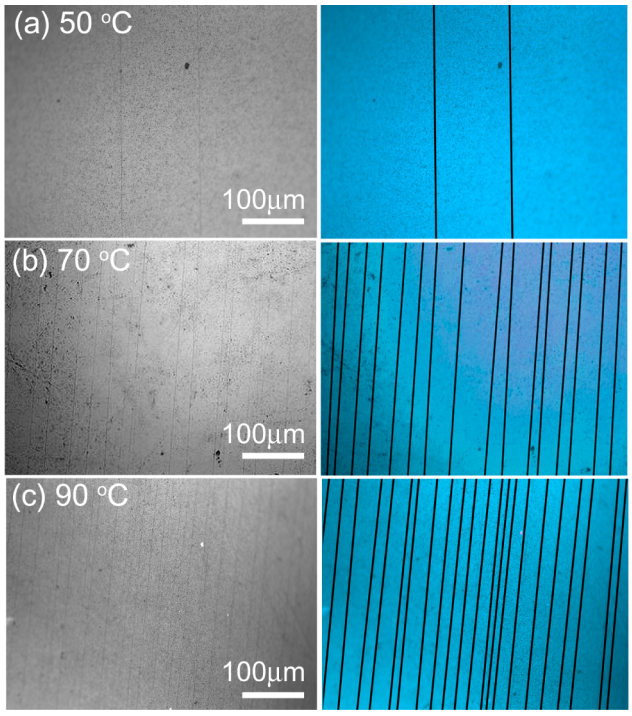

Figure 3. Optical micrographs showing cracks developed on the surface of PbS thin films deposited at different deposition temperatures of (a) 50, (b) 70, and (c) 90 °C on PET at a bending strain of ∼1.20%. The original images were photoedited in blue backgrounds for better contrast as seen on the right side.

along the pathway of grain boundary as the applied strain increased. It should be also mentioned, from our extra experiments, that no cracks were observed for the samples of ∼50 nm (in thickness) CdS/PET, ∼100 nm Al/PET, and ∼100 nm ITO/PET in the given range of applied strain. The results suggest that the formation of cracks is only applicable to the PbS layer within the range of applied strain.

Figure 4 shows the curves of crack density ρ with applied strain ε_a for the PbS films processed at different temperature.

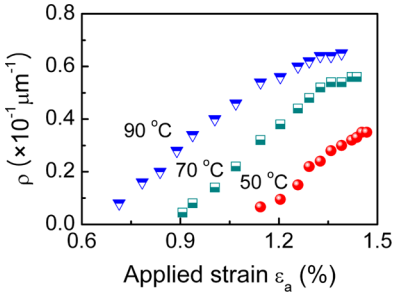

Figure 4. Variations in crack density as a function of applied strain for the PbS layers deposited at different temperatures of 50, 70, and 90 °C.

The additional parameters of the critical strain ε_c and saturated crack density ρ_s, which are extracted from the curves, are plotted as a function of deposition temperature as shown in Figure 5a,b. The minimum applied strain needed to initiate the cracks, which is so-called critical strain ε_c, was determined by extrapolating the ρ values into the x-axis of ε_a. The ε_c decreased with increasing deposition temperature, implying that the films deposited at a lower temperature can endure a higher strain

DOI: 10.1021/am507301c
ACS Appl. Mater. Interfaces 2015, 7, 4573−4578

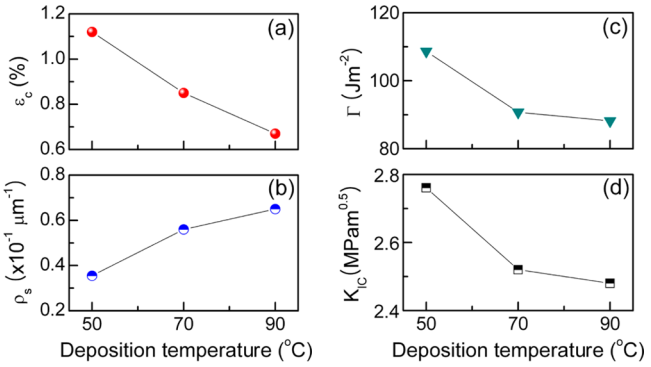

Figure 5. Plots of (a) critical strain ε_c, (b) saturated crack density ρ_s, (c) fracture energy Γ, and (d) mode I fracture toughness K_{IC} as a function of deposition temperature of PbS layer.

without mechanical failures. The highest ε_c value of ∼1.14% was obtained at 50 °C. The values were ∼0.90 and 0.71% for the PbS films deposited at 70 and 90 °C, respectively. The saturated crack density ρ_s exhibited the lowest value of 0.036 μm^{-1} at 50 °C, which is meaningful in that a higher stress does not create any further cracks once the saturation level is reached with the finer grains microstructure.

Understanding of the fracture behavior of flexible thin films is known to be complicated with interdependency of the physical parameters such as grain size, roughness, defects, and thickness. For instance, Changji et al.[27] and Balakrisnan et al.[28] have reported that pores and dislocations in films facilitate crack initiation, while grain boundaries provide an easy path for crack propagation. An extra energy is required for crack propagation if a higher effective density of grain boundary (or smaller grains) is present. It is postulated that the smaller grain size with more grain boundaries region affect positively the fracture behavior of the films as in the case of the lowest temperature of 50 °C. In addition, internal stress and its inhomogeneous distribution between protrusions on rough surfaces may influence critically the crack resistance of films.[29] Thus, smaller grains with least roughness are preferred to endure a higher applied strain on the flexible substrate.

Further insight into the fracture behavior of the PbS films were gained from evaluating the fracture energy Γ and mode I fracture toughness K_{IC}, which are depicted in Figure 5c,d as a function of deposition temperature. The Γ for the PbS films was calculated using the energy criterion proposed earlier for the multiple film cracking phenomenon.[30,31] Traditionally, the cracks can develop in the films if the change in the strain energy due to the cracking of the film is in equilibrium with the energy required for film cracking. Assuming a steady propagation of cracks,[30,31] Γ of the PbS thin film is given by

$$\Gamma = \frac{3E_f\varepsilon_c^2}{4\alpha}\left(\frac{1 - 2\nu_f\nu_s + \nu_s^2}{1 - \nu_f^2}\right) \quad (2)$$

where $\alpha = 1/t_f[3/(2\beta(1+\nu_s))(1/\beta + (1 - \nu_f^2)E_s/(1 - \nu_f\nu_s)E_f)]^{1/2}$, and ν_s and ν_f are the Poisson's ratio of substrate and PbS film, respectively. It is important to note that the determination of Γ (eq 2) involves the ratio of effective thickness of the substrate to the film, β. Using the procedure, as detailed elsewhere,[13] we determined the values of β as a function of deposition temperature, which enabled us to estimate Γ to a better degree of accuracy. The K_{IC} value was determined by the following relation:

$$\Gamma = \frac{K_{IC}^2}{E_f} \quad (3)$$

As observed from Figure 5c,d, both values of Γ and K_{IC} decrease gradually with increasing deposition temperature. The Γ values are ∼108.6, 90.7, and 88.1 J m^{-2} for the PbS films at 50, 70, and 90 °C, respectively. The higher fracture energy indicates relatively the less-brittle nature of the films. The obtained K_{IC} values of 2.4−2.8 MPa·m$^{1/2}$ are of the same order when compared to the reported values of 1.0 MPa·m$^{1/2}$ for ZnS.[32] Accordingly, it is conclusive that the enhanced fracture energy and fracture toughness are the main reasons for more resistive fracture behavior of the films processed at the lowest temperature of 50 °C.

Figure 6 shows the variations in the normalized solar cell parameters for the PbS absorber prepared at 50 °C at each applied strain. The solar cell was stressed in the tensile mode for 10 s at each bending radius and then released prior to the $J-V$ measurement. The normalized values were obtained by calculating the ratio of the changed value after bending to the initial value of the solar cell. The photovoltaic properties showed distinct dependence on the applied strain. The normalized FF and J_{sc} were initially stable up to an applied strain of ∼1.10% and then degraded dramatically above the strain, which is very close to the ε_c value of ∼1.14% for the PbS thin film. Accordingly, the degradation is assumed to be associated with the fracture behavior of PbS film observed in Figure 3. Note that no cracks were observed in the individual

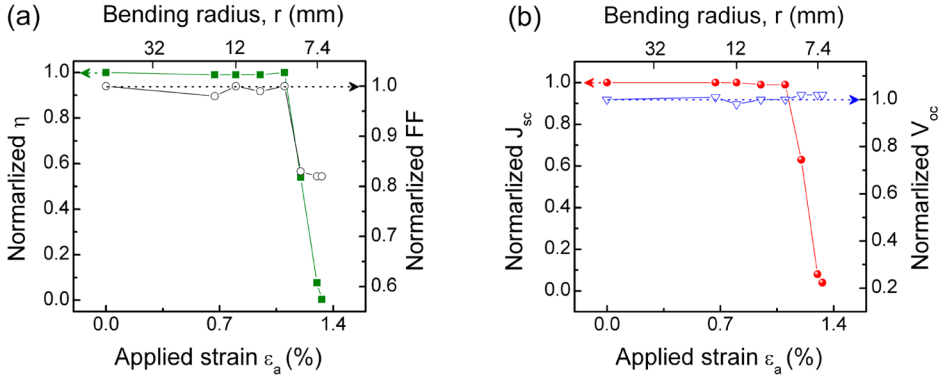

Figure 6. Variations in (a) conversion efficiency η and fill factor FF and (b) short-circuit current density J_{sc} and open-circuit voltage V_{oc} of the solar cells with increasing applied bending strain ε_a.

DOI: 10.1021/am507301c
ACS Appl. Mater. Interfaces 2015, 7, 4573−4578

fracture evaluation of Al/PET, CdS/PET, and ITO/PET under the same strain condition. The progress of the cracking seems to happen in the applied strain range from ~1.10 to ~1.33%, which corresponds to the degradation range of FF and J_{sc}. The decreases of FF and J_{sc} beyond the critical strain are primarily due to the increase in sheet resistance induced by cracks and hence to the limited transfer pathway of carriers. On the other hand, the V_{oc} is almost maintained at the initial value regardless of applied strain and generation of cracks. It is believed that multiple cracks in the PbS layer resulted in the formation of a number of cells of smaller area within the active cell area. Since all layers, apart from the absorber PbS film, maintained structural integrity, the resulting configuration still demonstrates near-constant V_{oc} even with evolved intercracks.

The degradation stages of the photovoltaic properties with applied strain are schematically represented in Figure 7. Up to a certain level, for example, ~1.10% applied strain in the case of 50 °C, promising mechanical endurance of the solar cells can be successfully maintained without affecting the photovoltaic properties (Figure 7a). As a strain above the critical level is applied, cracks are initiated and propagated with the substantial reduction of conversion efficiency due to the degraded J_{sc} and FF. This stage corresponds to the applied strain levels of ~1.10 to ~1.33% in this experiment (Figure 7b). A still higher value of applied strain beyond 1.33% resulted in the complete failure of the PbS layer and hence the device, as illustrated in Figure 7c.

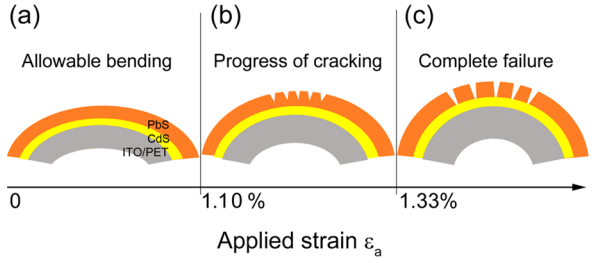

Figure 7. Schematic illustrations of the progress in mechanical failure of flexible PbS/CdS solar cells with applied strain levels in the case of 50 °C deposition: the stages of (a) allowable bending, (b) progress of cracking, and (c) complete failure of device.

CONCLUSIONS

Flexible PbS/CdS thin-film solar cells on the PET substrate are found to be mechanically resistive up to a certain level of applied strain under the tensile bending environment. The fracture behavior of the cells depends on processing temperature and thus on microstructural features such as grain size and surface roughness. As an example of such dependency, the PbS thin film deposited at the lowest temperature of 50 °C exhibits the lowest saturated crack density of 0.036 μm^{-1} and the highest critical strain of ~1.14%. The values of J_{sc} and FF are suddenly degraded with the progress of cracks, while V_{oc} is not much affected by the applied stress. The degradation of the photovoltaic properties with applied strain is likely controllable by achieving better microstructural features such as smaller grains and smoother surface.

ASSOCIATED CONTENT

Supporting Information

Standard deviation of the photovoltaic parameter. This material is available free of charge via the Internet at http://pubs.acs.org.

AUTHOR INFORMATION

Corresponding Author

*Phone: 82-2-2123-5848. E-mail: ycho@yonsei.ac.kr.

Author Contributions

§Equally contributed.

Notes

The authors declare no competing financial interest.

ACKNOWLEDGMENTS

This work was financially supported by the grants (Nos. 2011-0020285 and 2013-016711) from National Research Foundation of Korea (NRF) funded by the Korean government.

REFERENCES

(1) Jørgensen, M.; Norrman, K.; Krebs, F. C. Stability/Degradation of Polymer Solar Cells. *Sol. Energy Mater. Sol. Cells* **2008**, *92*, 686−714.
(2) Nelson, J. Organic Photovoltaic Films. *Curr. Opin. Solid State Mater. Sci.* **2002**, *6*, 87−95.
(3) Caballero, R.; Kaufmann, C. A.; Eisenbarth, T.; Unold, T.; Klenk, R.; Schock, H. W. High Efficiency Low Temperature Grown $Cu(In,Ga)Se_2$ Thin Film Solar Cells on Flexible Substrates Using NaF Precursor Layers. *Prog. Photovoltaics* **2011**, *19*, 547−551.
(4) Tiwari, A. N.; Romeo, A.; Baetzner, D.; Zogg, H. Flexible CdTe Solar Cells on Polymer Films. *Prog. Photovoltaics* **2011**, *9*, 211−215.
(5) Chirila, A.; Buecheler, S.; Pianezzi, F.; Bloesch, P.; Gretener, C.; Uhl, A. R.; Fella, C.; Kranz, L.; Perrenoud, J.; Seyrling, S.; Verma, R.; Nishiwaki, S.; Romanyuk, Y. E.; Bilger, G.; Tiwari, A. N. Highly Efficient $Cu(In,Ga)Se_2$ Solar Cells Grown on Flexible Polymer Films. *Nat. Mater.* **2011**, *10*, 857−861.
(6) Luther, J. M.; Gao, J.; Lloyd, M. T.; Semonin, O. E.; Beard, M. C.; Nozik, A. J. Stability Assessment on a 3% Bilayer PbS/ZnO Quantum Dot Heterojunction Solar Cell. *Adv. Mater.* **2010**, *22*, 3704−3707.
(7) Ju, T.; Graham, R. L.; Zhai, G.; Rodriguez, Y. W.; Breeze, A. J.; Yang, L.; Alers, G. B.; Carter, S. A. High Efficiency Mesoporous Titanium Oxide PbS Quantum Dot Solar Cells at Low Temperature. *Appl. Phys. Lett.* **2010**, *97*, 043106.
(8) Bhandari, K. P.; Roland, P. J.; Mahabaduge, H.; Haugen, N. O.; Grice, C. R.; Jeong, S.; Dykstra, T.; Gao, J.; Ellingson, R. J. Thin Film Solar Cells Based on the Heterojunction of Colloidal PbS Quantum Dots with CdS. *Sol. Energy Mater. Sol. Cells* **2013**, *117*, 476−482.
(9) Hernandez-Borja, J.; Vorobiev, Y. V.; Ramirez-Bon, R. Thin Film Solar Cells of CdS/PbS Chemically Deposited by an Ammonia-Free Process. *Sol. Energy Mater. Sol. Cells* **2011**, *95*, 1882−1888.
(10) Obaid, A. S.; Hassan, Z.; Mahdi, M. A.; Bououdina, M. Fabrication and Characterisations of n-CdS/p-PbS Heterojunction Solar Cells Using Microwave-Assisted Chemical Bath Deposition. *Sol. Energy* **2013**, *89*, 143−151.
(11) Yeon, D. H.; Lee, S. M.; Jo, Y. H.; Moon, J.; Cho, Y. S. Origin of the Enhanced Photovoltaic Characteristics of PbS Thin Film Solar Cells Processed at Near Room Temperature. *J. Mater. Chem. A* **2014**, *2*, 20112−20117.
(12) Mohanty, B. C.; Choi, H. R.; Choi, Y. M.; Cho, Y. S. Thickness-Dependent Fracture Behavior of Flexible ZnO:Al Thin Films. *J. Phys. D: Appl. Phys.* **2011**, *44*, 025401.
(13) Choi, H. R.; Mohanty, B. C.; Kim, J. S.; Cho, Y. S. AlN Passivation Layer-Mediated Improvement in Tensile Failure of Flexible ZnO:Al Thin Films. *ACS Appl. Mater. Interfaces* **2010**, *2*, 2471−2474.
(14) Grego, S.; Lewis, J.; Vick, E.; Temple, D. A Method to Evaluate Mechanical Performance of Thin Transparent Films for Flexible Displays. *Thin Solid Films* **2007**, *515*, 4745−4752.
(15) Chang, H. Y.; Yang, S.; Lee, J.; Tao, L.; Hwang, W. S.; Jena, D.; Lu, N.; Akinwande, D. High-Performance, Highly Bendable MoS_2 Transistors with High-k Dielectrics for Flexible Low-Power Systems. *ACS Nano* **2013**, *7*, 5446−5452.
(16) Sierrosa, K. A.; Cairns, D. R.; Abell, J. S.; Kukureka, S. N. Pulsed Laser Deposition of Indium Tin Oxide Films on Flexible Polyethylene

DOI: 10.1021/am507301c
ACS Appl. Mater. Interfaces 2015, 7, 4573−4578

Naphthalate Display Substrates at Room Temperature. *Thin Solid Films* **2010**, *518*, 2623−2627.
(17) Ni, J. L.; Zhu, X. F.; Pei, Z. L.; Gong, J.; Sun, C.; Zhang, G. P. Comparative Investigation of Fracture Behaviour of Aluminium-Doped ZnO Films on a Flexible Substrate. *J. Phys. D: Appl. Phys.* **2009**, *42*, 175404.
(18) Suo, Z.; Ma, E. Y.; Gleskova, H.; Wagner, S. Mechanics of Rollable and Foldable Film-on-Foil Electronics. *Appl. Phys. Lett.* **1990**, *74*, 1177−1179.
(19) Park, S. I.; Ahn, J. H.; Feng, X.; Wang, S.; Huang, Y.; Rogers, J. A. Theoretical and Experimental Studies of Bending of Inorganic Electronic Materials on Plastic Substrates. *Adv. Funct. Mater.* **2008**, *18*, 2673−2684.
(20) Zhu, X. F.; Zhang, B.; Gao, J.; Zhang, G.. P. Evaluation of the Crack-Initiation Strain of a Cu-Ni Multilayer on a Flexible Substrate. *Scr. Mater.* **2009**, *60*, 178−181.
(21) Lobontiu, N.; Garcia, E. *Mechanics of Microelectromechanical Systems;* Springer: New York, 2005.
(22) Bass, M. *Handbook of Optics: Devices, Measurement, and Properties,* 2nd ed.; McGraw-Hill: New York, 1995.
(23) Gaith, M.; Alhayek, I. Correlation between Overall Elastic Stiffness, Bulk Modulus and Interatomic Distance in Anisotropic Materials: Semiconductors. *Rev. Adv. Mater. Sci.* **2009**, *21*, 183−191.
(24) Neerinck, D. G.; Vink, T. J. Depth Profiling of Thin ITO Films by Grazing Incidence X-ray Diffraction. *Thin Solid Films* **1996**, *278*, 12−17.
(25) Pawar, S. B.; Shaikh, J. S.; Devan, R. S.; Ma, Y. R.; Haranath, D.; Bhosale, P. N.; Patil, P. S. Facile and Low Cost Chemosynthesis of Nanostructured PbS with Tunable Optical Properties. *Appl. Surf. Sci.* **2011**, *258*, 1869−1875.
(26) Preetha, K. C.; Remadevi, T. L. Behavior of Chemically Deposited PbS Thin Films Subjected to two Different Routes of Post Deposition Annealing. *Mater. Sci. Semicon. Process.* **2013**, *16*, 605−611.
(27) Changji, H.; Zhenhui, H.; Weichun, F.; Qi, Z. Influence of Deposition Pressure on the Adhesion of ZnO Thin Films Deposited by Cathodic Vacuum Arc Deposition on Polyimide Foil Substrates. *J. Phys. D: Appl. Phys.* **2009**, *42*, 185303.
(28) Balakrisnan, B.; Chum, C. C.; Li, M.; Chen, Z.; Cahyadi, T. Fracture Toughness of Cu-Sn Intermetallic Thin Films. *J. Electron. Mater.* **2003**, *32*, 166−171.
(29) Park, J. W.; Kim, G.; Lee, S. H.; Kim, E. H.; Lee, G. H. The Effect of Film Microstructures on Cracking of Transparent Conductive Oxide (TCO) Coatings on Polymer Substrates. *Surf. Coat. Technol.* **2010**, *205*, 915−921.
(30) Hsueh, C. H.; Wereszczak, A. A. Multiple Cracking of Brittle Coatings on Strained Substrates. *J. Appl. Phys.* **2004**, *96*, 3501−3506.
(31) Hsueh, C. H.; Yanaka, M. Multiple Film Cracking in Film/Substrate Systems with Residual Stresses and Unidirectional Loading. *J. Mater. Sci.* **2003**, *38*, 1809−1817.
(32) Klocek, P.; Stone, L. E.; Boucher, M. W.; DeMilo, C. Semiconductor infrared optical materials. *Proc SPIE. Infrared Optical Materials VI* **1988**, *929*, 65−78 DOI: 10.1117/12.945853.

DOI: 10.1021/am507301c
ACS Appl. Mater. Interfaces 2015, 7, 4573−4578